

Chapter 21

Surface Modification and Bioconjugation of Nanoparticles for MRI Technology



M. Azam Ali and Mohammad Tajul Islam

Abstract Nanomaterials (NPs) with precise biological functions have considerable potential for use in biomedical applications. Surface modification is one of the effective routes to impart such desired and precise biological functions to NPs. Introduction of various reactive functional groups on the surface of NPs are required to conjugate a spectrum of contrast agents (CAs), for the targeted imaging such as magnetic resonance imaging (MRI). Current state in surface modification of NPs for preparing CAs of MRI is summarized in this chapter. Chemistries involved in the bioconjugation and surface modification are discussed. Chemical and bioconjugate reactions to transform the surface of NPs such as silica NPs, gold NPs, and gadolinium NPs are highlighted. Coating is another important approach to enhance the functionalities of CAs for MRI application, therefore, light is thrown on the coating mechanism of organic polymers including dextran, chitosan, and copolymers.

Keywords Surface modification · Bioconjugation · Nanoparticles · Contrast agent · Magnetic resonance image

1 Introduction

Imaging techniques, which detect lesion information (e.g., type, location, and stage) offer tremendous opportunities both for clinical diagnostics and as a research tool [1]. Among all existing imaging techniques, magnetic resonance imaging (MRI) has emerged as one of the most powerful diagnostic tools in biomedicine primarily due to its exquisite soft tissue contrast, high spatial resolution, lack of ionizing radiation, unlimited signal penetration depth, and wide clinical applicability [2].

M. A. Ali (✉)

Centre for Bioengineering and Nanomedicine, Department of Food Science,
Division of Sciences, University of Otago, Dunedin, New Zealand
e-mail: azam.ali@otago.ac.nz

M. T. Islam

Centre for Materials Science and Technology, University of Otago, Dunedin, New Zealand

Another advantage of MRI is that it can obtain real-time images of the internal anatomy and physiology of living organisms in a noninvasive manner. Furthermore, MRI provides information not possible to access with other imaging modalities. Recently, three-dimension (3D) MRI has been shown to be much useful in the evaluation and diagnosis of brain and neural tissue anatomy using a single acquisition technique. Therefore, it has been extensively used for imaging brain and central nervous systems, for assessing cardiac function, and for detecting abnormal tissues such as tumors [2].

An MRI is the collection of pixels or voxels representing the nuclear magnetic resonance (NMR) signal intensity of the hydrogen atoms in water and fat of the body area of living organisms being imaged. MRI scanner applies a strong magnetic field around the area of the body to be imaged. The hydrogen nuclear spins are aligned in the direction of the external magnetic field (Fig. 21.1a). Figure 21.1b shows that when a resonant radiofrequency wave (5–100 MHz) is applied, some protons with low energy absorb the electromagnetic energy and flip their spin. After removal of the radio frequency, the protons gradually return to their normal spin. Protons simultaneously release the energy in the form of radio waves during resuming their original state, which are measured by receivers and made into the MR images. Returning process of the protons to their original state is known as relaxation. Relaxation is measured in two directions, longitudinal and transverse, and characterized by the time constants: spin–lattice relaxation time T_1 or spin–spin relaxation time T_2 , respectively [3, 4].

However, MRI's inherent low sensitivity, little difference between normal and abnormal soft tissues in relaxation time, and resulting contrast usually provides poor anatomic descriptions, which hampers the visualization of subtle changes in tissues. Therefore, additional supplements have been used for further improvement of the contrast of imaging, and more accurate detection and diagnosis. The most

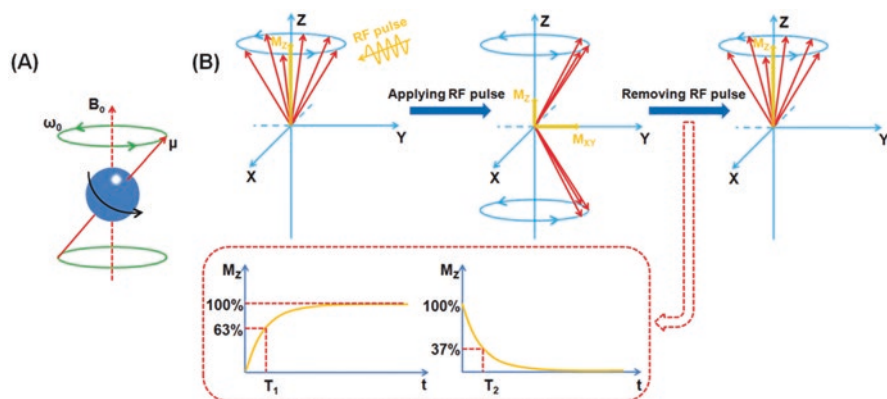


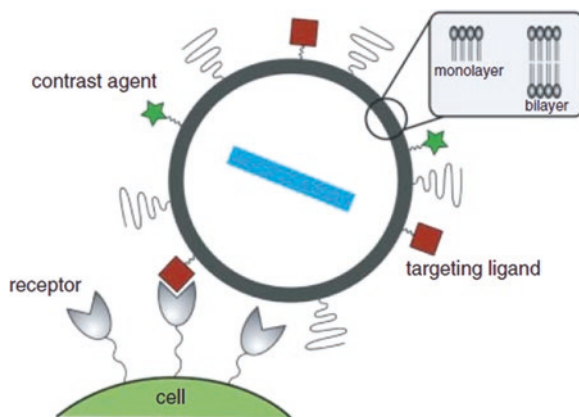
Fig. 21.1 Schematic illustration of the mechanisms of MRI. (a) Protons precessing under an external magnetic field B_0 . (b) After the introduction of the RF pulse, protons are excited, with relaxation occurring following removal of the RF pulse. And the graphical representation of T_1 relaxation and T_2 relaxation. Reproduced from [3] with permission of Royal Society of Chemistry

effective supplement is a chemical compound known as a probe or a CA. CA is introduced to a living body prior to MRI scanning to enhance the signal difference between the region of interest (disease) and the background (normal tissues). In general, contrast agents can make the signal difference by modifying the water proton relaxation rates when present in micromolar concentrations, although recent advances can produce nanomolar detection levels [5]. Moreover, the interrelation between the contrast agent and the biological system often reveals biological and functional information [2].

Merbach et al. [6] reported in their book in 2013 that approximately 35% of clinical MRI scans took the assistance of CAs, although this is dependent on the type of CA, which is expected to increase signal intensity and/or imaged performances further with the emergence of novel and more effective CAs compared to commercially available CAs at present. CAs can be categorized into four class based on the MR mechanism to generate signal: T1, T2, PARACEST (paramagnetic chemical exchange saturation transfer), and hyperpolarization [1]. T1 and T2 are more commonly used CAs amongst these four. T1 contrast agents are known as positive contrast agents since they increases the signal intensity in T1-weighted images by shortening T1. On the other hand, T2 contrast agents reduces the signal intensity in T2-weighted images and hence called negative contrast agent [4]. One of the most common T1 CAs employed in clinical imaging is paramagnetic gadolinium ion complex while superparamagnetic iron oxide nanoparticle (SPION) is the typical example of T2 MRI contrast agent [2]. Unfortunately, CAs are not free from limitations. Being small molecules CAs shows limited efficacy. As a result, to obtain desired contrast relatively high dose of CAs is required [7]. To overcome this limitation, CAs were incorporated into nanoparticles via bioconjugation (Fig. 21.2). Nanoparticle acts as a carrier for the CAs and improve the relaxation time thereby efficiently amplify the contrast signal at locations of interest.

The synthesis of NPs requires an organic solvent or a complex aqueous mixture, which is unfortunately not compatible with direct biomedical use. Therefore, surface modification is essential to get colloidal stable NPs at physiological pH as well

Fig. 21.2 Schematic representation of a lipid-based nanoparticle, which binds to a cell-surface receptor. The nanoparticle carries contrast agents (green), a payload of drug (blue), and is equipped with targeting ligands (red) for specific receptor recognition. Reproduced from Nicollay et al. (2013) with permission of Wiley



as targeting abilities and additional functionalities that demonstrate biocompatibility to the body tissues. The initial surface functionality can be introduced during synthesis of NPs. Otherwise the surface layer can be modified after synthesis either by chemical modification of the initial ligand or by complete ligand exchange. Hundreds of thousands of CAs such as gadolinium ions or iron oxides can be loaded per nanoscale CA structure. Furthermore, surface modification of nanoscale CAs can introduce various functionalities, such as targeting ligands for tumor targeting, dyes for multimodal imaging and drugs for constructing therapeutic nanoplatforms [3]. In this chapter, we introduce and report the recent developments of surface modification of various CAs including bioconjugation of nanoparticles for MRI technology.

2 Surface Modification Chemistry

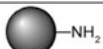
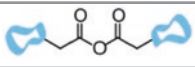
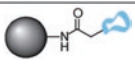
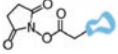
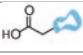
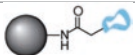
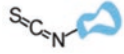


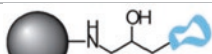
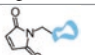
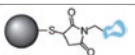
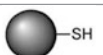
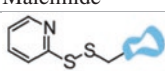
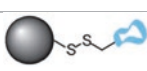
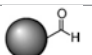


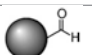
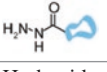
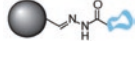
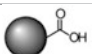
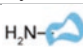
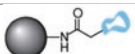
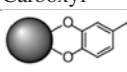
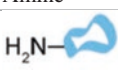
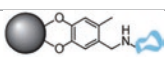

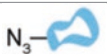
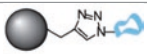
2.1 Covalent Linkages

Covalent linkage is one of the strong and stable bonds formed between functional groups found on the NP surface and conjugated ligands. Usually, these functional groups such as amino, carboxylic acid, and thiol groups are added to the NP surface via its polymer coating. Both the type and number of functional groups on each NP can be controlled during the coating of polymers. Functional groups are present either on the body of the natural or synthetic polymers chain (such as chitosan, dextran, PEI) or at their terminal ends (such as PEG). At the same time, total number of reactive groups can also be customized by adding specific number of binding sites per polymer chain. For example, superparamagnetic iron oxide nanoparticles (SPIONs), 38 nm, in particular have been extensively investigated as novel magnetic resonance imaging (MRI) CAs which coated with dextran have been reported with 62 reactive amino groups per NP [8]. While a larger SPION (64 nm) coated with PEG was reported to have 26 reactive amino groups per NP [9]. These same chemical groups are also found on the targeting, optical, or therapeutic agent to be covalently attached. To link the functional groups a host of chemistries are available, which are subdivided into direct reaction (Table 21.1), click chemistry (Table 21.1), and linker strategies (Table 21.2).

2.1.1 Direct Nanoparticle Conjugation

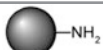
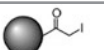

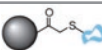
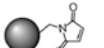
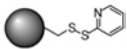

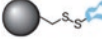
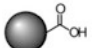
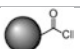

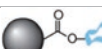
Direct reaction strategies are particularly suitable for small molecule conjugation. As listed in Table 21.1, functional groups such as amine, sulfhydryl, aldehyde, carboxyl, and active hydrogen functional groups present at the NP surfaces can be directly bonded or linked to reactive ligands by a number of reactions schemes, for example Mannich reaction, Michael addition, Schiff-base condensation and epoxide opening. A linkage reaction between the functional groups and ligand can also be possible, which is facilitated with the help of catalysts. In one notable study [8], 146 different small molecules were conjugated to 10-kDa dextran-coated

Table 21.1 Direct nanoparticle conjugation

Nanoparticle	Ligand	Conjugate	Reaction
 Amine	 Anhydride		Amide bond formation
	 Succinimidyl ester		
	 Carboxylic acid ester		
	 Isothiocyanate		
 Epoxide	 Epoxide		Epoxide opening
	 Maleimide		Michael addition
 Sulfhydryl	 Pyridyl disulfide		Substitution
	 Aldehyde	 Amine	
 Aldehyde	 Hydrazide		Imine formation
	 Carboxyl	 Amine	
 Active hydrogen	 Amine		Mannich reaction
 Alkyne	 Azide		Click chemistry

monocrystalline magnetic NP in array format to impart water solubility, conjugatability, biocompatibility, and chemical diversity. On an average, 60 small molecules (MW < 500 Da) with the chemical functional groups of primary amines, alcohols, carboxylic acids, sulfhydryls, and anhydrides were attached per 38-nm nanoparticle. Fourteen compounds showed significant uptake into cancer cells (up to 160×10^6 nanoparticles per cell for the most efficient compounds) for early detection of

Table 21.2 Linker chemistry conjugation

Nanoparticle	Linker chemistry	Ligand	Conjugate
 Amine	 Iodoacetyl		
	 Maleimide		
	 Pyridyl disulfide		
	 Carboxyl		
 Thionyl chloride			

pancreatic cancer. The authors concluded that the efficacy of prepared materials might be attributed to the multivalent nature of the surface molecules (60 ligands per nanoparticle). However, the efficiency of these chemistries varies with the functional groups. Functionalized NPs obtained from direct conjugation methods are prone to intercalating or cross-linking, with the exception of amine functional groups. Specifically, disulfide linkage formation between NPs may be the reason for the cross-linking. Another reason might be binding amongst multiple NPs and a single ligand containing multiple amino functional groups. Moreover, there is a need for initial modification prior to conjugation since biomolecules are not natively reactive with NPs. Modification of biomolecules involves the risk of loss of biocompatibility and bioactivity. However, Schellenberger et al. [10] reported that only precise, limited modifications can be possible without losing the bioactivity. Therefore, care should be taken during chemical modification to limit the loss of biofunctionality and bioactivity. Unfortunately, glutaraldehyde, a common direct conjugation agent, has limited applicability for biomolecule-NP attachment as it denatures proteins and peptides. Tetraethylene glycol (TEG)-based phosphonate ligands were introduced in stable superparamagnetic iron oxide nanoparticles via both direct conjugation and ligand exchange process. The direct conjugation has found less toxic to cell whereas ligand exchange process lead to NP with greater magnetic properties [11] that illustrate effective performance for MRI imaged.

2.1.2 Click Chemistry

Sharpless et al. in the year 2005 developed “click” chemistry to generate substances by joining small units together with heteroatom links (C–X–C) [12]. Table 21.1 shows Cu-catalyzed azide–alkyne chemistries. The intention of the development of

click chemistry was to give an easier route for conjugations between bioactive surfaces and less harsh environment to biomolecule ligands [13]. Click reactions have several advantages such as they are fast, efficient, take place in aqueous environment at relatively neutral pH (mild reaction conditions). Bonds formed by click chemistry are water-soluble and obtained biocompatible linkages are electronically similar to amide bonds [14]. This method of attachment offers several unique features over other direct conjugation strategies. Specific conjugation at the desired location(s) on the reactive moiety is obtained as azide and alkyne reactive groups are highly specific to each other, and do not react with most functional groups. In addition, bonds formed by click chemistry are highly stable whereas amide bonds and disulfide linkages formed by other direct conjugation techniques are prone to cleavage by hydrolysis and reduction, respectively. Moreover, there is a very little risk of cross interaction among moieties at the NP surface. This is because of the rigidity of formed linkages, which helps to maintain conformation of reacted moieties in place. Thanks to those features for which production of highly oriented linkages, capable of optimal reaction activity and efficiency, is possible. Therefore, click chemistry is considered as a desired technique where orientation and stability of linkages are particularly important [15]. Click chemistry was implemented with SPIONs under mild reaction conditions with a reaction time of 5–8 h. Orthogonal to thiol- and amine-containing targeting motifs were effectively bound with NP at an efficiency of >90%, and the resultant linkages were stable in the complex in-vivo environments of the blood and tumor milieu [16]. However, there are some drawbacks of click chemistry in its implementation. Cu catalyst is required to advance the reaction, which may disturb the biocompatible nature of the formed linkage. A number of disorders such hepatitis, neurological disorders, kidney diseases, and Alzheimer's disease were found to be linked with the excessive Cu consumption [14]. To minimize this proper purifications are required to remove all of the catalyst from magnetic nanoparticle (MNP) solutions before use. Another issue is biodegradation. The highly stable linkages formed may render nonbiodegradability to MNP.

2.1.3 Linker Chemistry

Covalent linkage by linker chemistry can control the molecular orientation of bound ligands, which is very important to protect the functionality of targeting ligand. Cleaving of linkers selectively is possible for some applications such as ligand quantification, controlled release of drugs. Amine or carboxylic acid functionalized SPION surfaces have been modified with heterobifunctional molecules such as iodoacetyl, maleimide, pyridyl disulfide, and thionyl chloride followed by the reaction with reactive ligands as shown in Table 21.1. In this approach, usually a linker molecule is used to link or bind the functional group of a SPION surface with the sulfhydryl (SH) of a biomolecule. Cystine amino acid residues are suitable target for reaction in case of biomolecules containing proteins and peptides. If reactive cystine amino acids are not present, terminal primary amine groups can be thiolated with heterofunctional linker such as *N*-succinimidyl-*S*-acetylthioacetate [17]. Alternatively, a free sulfhydryl group can be grafted to chlorotoxin through

modification with Traut's reagent (2-mercaptoethylamine-HCl reagents) [18]. However, in the latter case to avoid any risk of undesired cross-linking prior to reaction with NPs, the introduced sulfhydryl group initially needs to be protected.

Oligonucleotide based molecules such as siRNA biomolecules containing sulfhydryls was synthesized and conjugated to SPIONs via linker chemistry. In brief, Cy5.5 succinimide ester was conjugated with SPION followed by another conjugation with a heterobifunctional cross-linker, *N*-succinimidyl 3-(2-pyridyldithio) propionate [19].

Complex biological molecules or biomacromolecules with multiple reactive sites can be suitably conjugated using linker chemistry method. To improve the MRI probe for efficient detection of gene expression, SPIONs were linked with targeting ligands using both linker chemistry and direct conjugation by Högemann et al. [20]. In linker chemistry method, SPIONs with a cross-linked dextran coat were conjugated to transferrin (Tf) through the linker molecule *N*-succinimidyl 3-(2-pyridyldithio)propionate. Direct conjugation was carried out by oxidative activation of the dextran coat with subsequent reduction of Schiff's base. The comparison study revealed that conjugation using linker chemistry provided approximately four-times Tf molecules attached per SPION. The resulted SPION showed 10 times more enhancement of binding and uptake by cells, and 16 times better for imaging gene expression. Higher number of active Tf proteins at the NPs surface obtained by linker chemistry provided better control over the binding sites used in ligand conjugations. Another advantage of linker chemistry is it minimizes the risk of adverse effect on bioactivity of the protein as relatively a milder reactive condition of this chemistry limits the oxidative conditions.

Disulfide linkages and reaction byproduct produced by Pyridyl disulfide (PD) heterobifunctional linkers are cleavable and quantifiable, respectively. Quantification enables the possibility of evaluation of reaction efficiency. Schellenberger et al. [21] demonstrated this utility in the preparation of SPIONs conjugated with annexin V by PD linker molecule. If the application medium is reducing environment then other stable linkers such as iodoacetyls or maleimides should be used as the bonds formed via PD linker chemistry are sensitive to reducing environments.

Amide linkages are obtained through *N*-ethyl-*N'*-(3dimethylaminopropyl)-carbodiimide hydrochloride (EDAC)/*N*-hydroxysuccinimide (NHS) linkers where SPIONs decorated with carboxylic acid groups covalently bonded to biomolecules bearing primary amines. This approach has been used in the attachment t-Boc-protected folic acid [22] to SPIONs. Figure 21.3 shows another example of EDAC/NHS linker chemistry for the linking of aptamers with SPION [23]. EDAC/NHS can effectively attach molecules that have only one amino group. However, in case of multiple amines it is difficult to control the binding orientation of ligands, often resulting into inactivation of the ligands. Therefore, sulfhydryl-based linker chemistry is the preferred conjugation technique for the attachment of peptides, proteins, antibodies, and enzymes to amino-decorated SPIONs.

There are some drawbacks of linker chemistry such as complexation of covalent bond formation between NPs or ligands, which needs stepwise NP modification prior to ligand attachment. Some linker chemistries have low yield due to the long reaction times and purifications between each step.

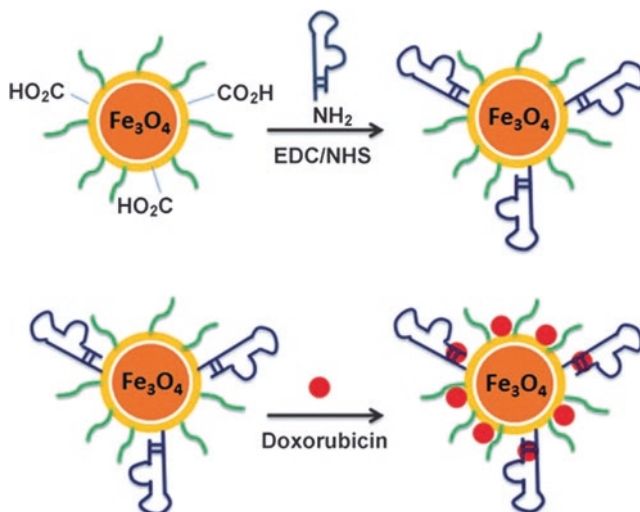


Fig. 21.3 Schematic illustration of the TCL-SPION-Apt bioconjugate system. Adapted from [23] with permission of Wiley

Table 21.3 Physical interaction attachment

Nanoparticle	Ligand	Functionalized nanoparticles	Reaction
 Charged surface			Electrostatic interaction
 Hydrophobic surface			Hydrophobic interaction
 Biotinylated			Biotin-avidin interaction

2.2 Physical Interactions

Physical interactions found in conjugation are mainly electrostatic, hydrophilic/hydrophobic, and affinity interactions that largely occurred onto the NPs surfaces (Table 21.3). These physical interactions offer several advantages. It allows for the design of very small targeted particles (<20 nm) on the basis of anionic nanoparticles. This surface modification and coupling techniques overcome the main disadvantages of SPIONs compared to gadolinium based probes. Other advantages of this coupling

technique include rapid binding, high efficiencies, and highly economic as no need for intermediate modification steps. Electrostatic interactions were found to be highly sufficient in complexing of plasmid DNA onto SPIONs. SPIONs were coated with cationic polymers of polyethylenimine (PEI) to be used as complexation agents for negatively charged plasmid DNA molecules [24]. The conjugate (SPION-PEI) is capable of assembling plasmid DNA into NPs with diameters ~ 100 nm and protecting the DNA from nuclease degradation. Highly efficient cells transfection with low toxicity was observed from the SPION-polyplexes. In addition, the T2 relaxation time of water was enhanced [25]. Electrostatic interactions were successfully applied to bind cationic proteins to an anionic SPION surface. The electrostatic attraction took place between the strongly positively charged peptide protamine and the anionic citrate shell of the electrostatically stabilize SPIONs [26].

Jain et al. [27] investigated the drug delivery and MRI properties of oleic acid-coated iron-oxide and pluronic-stabilized MNPs. Doxorubicin and paclitaxel drugs were loaded (alone or in combination) in MNPs with an efficiency of 74–95% and the drug release was sustained. Incorporated drugs showed marginal effects on physical (size and zeta potential), and magnetization properties of the MNPs. Hydrophobic interactions were the physical interaction force between the hydrophobic layers of drug and MNPs. However, hydrophobic interactions make NP sensitive to environmental conditions, decrease the T1 relaxation of MNPs slightly, and bring low control over molecular orientation of bound ligands. As a result, attachment of targeting ligands through these strategies is unattractive. On the other hand, affinity interactions, which is another form of physical interaction, can effectively bioconjugate targeting ligands to SPIONs [28]. Table 21.3 shows that SPION surfaces modified with streptavidin can be specifically bound to biotinylated molecules. The linkage formed is the strongest and highly stable of all noncovalent linkages chemistries. Unlike hydrophobic and electrostatic interactions, environmental conditions such as changes in pH, salinity, or hydrophilicity do not affect the affinity binding. Using this strategy Gunn et al. [29] produced high-affinity multivalent display of targeted SPIONs for immunotherapy applications.

3 Surface Chemistry Dependent on NP Material

The main chemistries developed for surface functionalization of silica NP, gold NP, quantum dots, and carbon nanotubes are summarized here. The most important reactions and recent highlights are mainly reported below, with a focus on the relationship between nanomaterial composition and functionalization method.

3.1 Silica NPs

One of the most widely used methods for the surface functionalization of NPs is silica coating. Silica NPs have gained interest for bioimaging application due to their straightforward and size-controlled synthesis, chemical and physical

stabilities, large surface area, hydrophilic surface, and well-defined surface chemistry. The same physicochemical properties also make them suitable as a protecting shell material for a wide number of nanomaterials. Such silica shells protect NPs against chemical and biochemical degradations, release of toxic ions, and activation of immune response along with hydrophilic, biocompatible and chemically active surfaces.

As-synthesized silica NPs possess highly hydrophilic surfaces, this is due to the presence of the silanol (Si-OH) groups on the surface of the particle, which make them one of the friendliest nanomaterials for biomedical applications including bioimaging. Furthermore, these silanol groups can chemically react with various reagents to render the silica hydrophobic. However, desired surface functional groups are required for the conjugation of contrast agents to the surface as well as inside the pores of silica NPs. The cocondensation process during the preparation of silica or post-synthesis surface modification is used to introduce reactive functional groups such as a primary or a secondary amino, carboxyl, hydroxyl, alkyl halogen, or azide group [30]. As-synthesized silica nanoparticles contain ample hydroxyl groups, which can be conjugated with isocyanates to form urethanes or carboxylic acids to form esters. Thiol-functionalized silica NPs can be obtained from the condensation of 3-mercaptopropyltriethoxy silane or its analogues with silanol groups on the surface of silica NPs. Thiol functionalized silica NPs can be further conjugated with gold nanoparticles, or biomolecules such as proteins, antibodies, peptides, polymers by reductive addition, disulfide coupling, or maleimide reaction. Thiol and maleimide functionalized molecules react with thiol groups on the surface of silica nanoparticles to form redox-active disulfide bonds, and thioether bonds, respectively [31]. Silica NPs can also be functionalized by introducing azide groups followed by click chemistry with alkyne substituted molecules.

Applications of silica NPs in bioimaging are vast due to their ability to accommodate MRI contrast agents and drug/DNA molecules to their adaptable surface and pores [32]. Chemical modifications of the surface of silica NPs can be conveniently chosen during the incorporation of various contrast agents. Various probes can be conjugated to silica NPs and efficiently delivered in different cell lines or injected in vivo [33]. Silica NPs can be coated with a dense layer of paramagnetic and PEGylated lipids in absence of coupling agent. The silica nanoparticles carrying a quantum dot in their center and were made target-specific by the conjugation of multiple $\alpha\beta3$ -integrin-specific RGD-peptides to enable their detection with both fluorescence techniques and MRI [34]. Figure 21.4 shows that higher signal intensity for the pellet of cells incubated with the RGD-conjugated Q-SiPaLCs (the bright white circle) was obtained as compared to the control cell pellets (gray circles). The differences in relaxation rate R1 ($1/T1$) clearly demonstrate the effective and specific targeting of this NPs agent to angiogenically activated endothelial cells (Fig. 21.4b). Core-shell-structured mesoporous silica nanoparticles was also synthesized to decrease T2 relaxation [35].

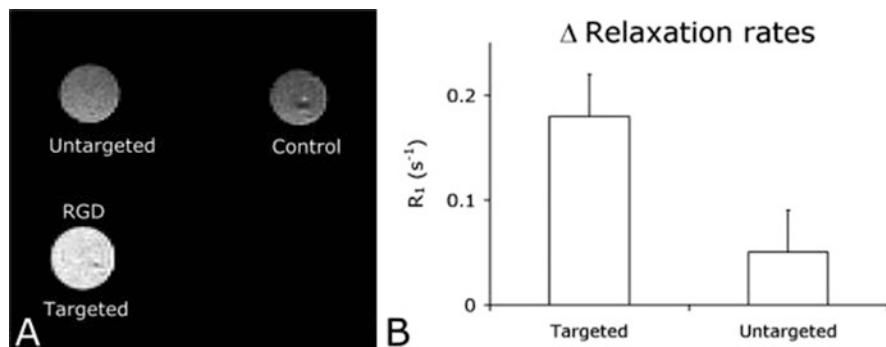


Fig. 21.4 (a) T1 weighted MRI of the different cell pellets revealed specific uptake of the targeted nanoparticles. (b) Difference in relaxation rates (R_1) of the targeted and untargeted cell pellets compared to the relaxation rate of the control cell pellet. The differences in relaxation rate reflect the concentration of contrast agent in the untargeted and targeted cell pellets. Reprinted with permission from [34]. Copyright (2008) American Chemical Society

3.2 Gold NPs

Colloidal gold nanoparticles are highly suitable for bioimaging owing to their brilliant color and size-and-shape-dependent tunable surface plasmon. Other promising properties of gold NPs for bioimaging are the straightforward synthesis, well-defined surface chemistry, nontoxic nature, and the large one- and two-photon absorption cross sections. Optical and electronic properties of gold nanoparticles for bioimaging applications can be tuned by modifying their surface chemistry and aggregation state.

As-synthesized gold NPs do not have many types of surface capping ligands and functional groups. Therefore, gold NPs need to be decorated with desired functional groups via ligand exchange reactions and chemical modifications for enabling them for MRI applications. Usually the surface of as-synthesized gold NPs contains alkane thiols capping ligands. Giersig and Mulvaney [36] first reported that thiol plays an important role to facilitate the exchange reaction since it has high affinity for gold. The Au–S bond is relatively strong ($H = 253.6$ kJ/mol), though it is not as stable as the Si–O covalent bond ($H = 799.6$ kJ/mol) [37]. This makes the functionalization task easy by ligand exchange but colloidal stability overtime under highly saline conditions or in a biological environment is limited. Colloidal stability seems to be closely related to the ligand packing [38]. To overcome this limitation with multiple thiol groups have been synthesized on ligands to get more stable form, such as dihydrolipoic acid (DHLA) [39] or thioctic acid [40]. Multiple binding points provide increased stability allowing for more densely packed ligands where sulfur anchoring groups are structurally constrained [41]. Diazonium salts chemistry is another possible option, however, the drastic conditions of the in situ diazonium formation limits its potential application [42]. Gold can be coated via a reduction of gold precursors on SPIONs of selected sizes as seeds [43]. In addition to core–shell structures, gold coating on SPIONs with heterostructures are widely used in medical practice (Fig. 21.5) [44].

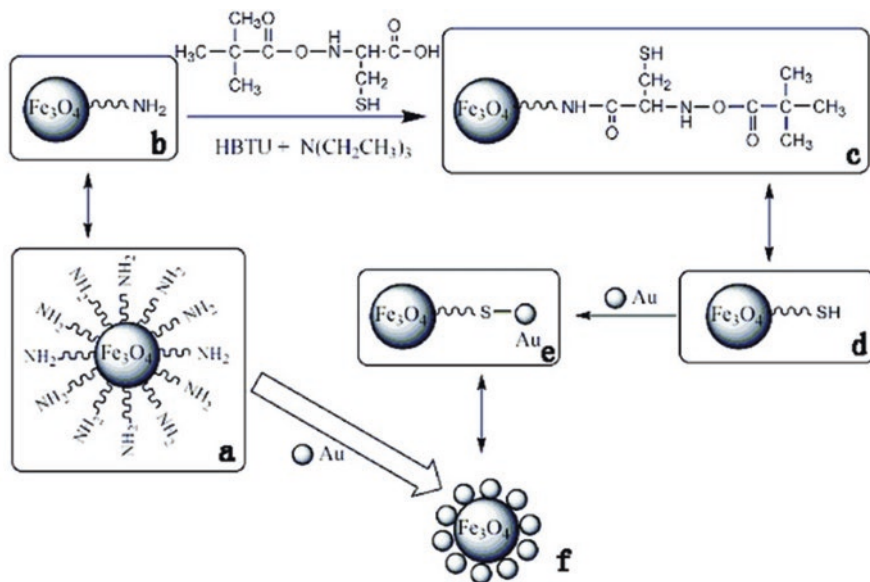


Fig. 21.5 Schematic illustration of bifunctional Au-Fe₃O₄ nanoparticle synthesis. Amino-functionalized Fe₃O₄ nanoparticles [(a), simplified as (b) for the convenience of illustration] were first modified by Boc-L-cysteine to have surface thiol groups [(c), simplified as (d)]. Gold nanoparticles were then conjugated onto the surface of Fe₃O₄ nanoparticles to form the expected Fe₃O₄-Au bifunctional nanoparticles [(f), simplified as (e)]. Reprinted with permission from [44]. Copyright (2007) American Chemical Society

3.3 Gadolinium NP

One promising new direction in the development of MRI contrast agents involves the labeling and/or loading of nanoparticles with gadolinium (Gd). Gadolinium ion (Gd³⁺) and calcium ion (Ca²⁺) have very similar ionic radius although former has higher positive charge. Ca²⁺-requiring proteins such as calmodulin, calsequestrin, and calexitin cannot distinguish (Gd³⁺) and (Ca²⁺). Consequently, Gd³⁺ would quickly bind to Ca²⁺ channels [45]. Free or unchelated gadolinium ions have toxic effect on most biological systems and cannot be administered to a patient in their aqueous form. Potential toxicity of the gadolinium ions can be suppressed by binding them with a strongly coordinating ligand for clinical examinations. Currently approved gadolinium-based CAs for clinical MRI are given in Fig. 21.6. These existing forms of gadolinium ions can directly constitute NPs for MRI CAs. Gadolinium ion can also be used as a chelate incorporated into the nanocarriers.

There is a range of polymeric micelles designed to develop gadolinium-based nanoscale CAs for MRI. The most commonly polymeric micelles is developed by conjugating the gadolinium chelates to the hydrophilic layer, which modifies the relaxivity properties favorably. Nanoscale micelles based on poly(L-glutamic acid)-

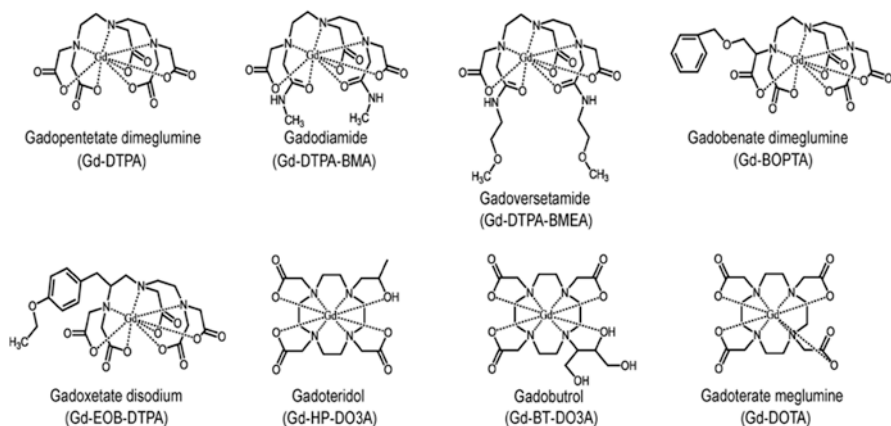
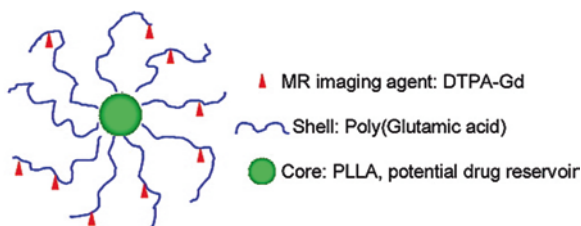


Fig. 21.6 Chemical structure of currently marketed gadolinium-based MRI CAs. Reproduced from [3] with permission of Royal Society of Chemistry

Fig. 21.7 Schematic model of the micellar structure with DTPA-Gd chelated to the shell layer. Adapted from with permission [46]. Copyright (2008) American Chemical Society



b-polylactide block copolymer was produced with paramagnetic Gd³⁺ ions chelated to their shell. The metal chelator *p*-aminobenzyl-diethylenetriaminepenta(acetic acid) (DTPA) was used to readily conjugate to the side chain carboxylic acids of poly(L-glutamic acid). The resulting DTPA-Gd chelated spherical micelles (Fig. 21.7) exhibited significantly higher spin–lattice relaxivity than a small-molecular-weight MRI CA [46]. A suitable chelating agent such as 1,4,7,10-tetraazacyclododecane-1,4,7,10-tetraacetic acid mono (*N*-hydroxysuccinimide ester) (DOTA-OSu) was used as an active chelating agent to conjugate gadolinium ions with a block copolymer, PEG-*b*-poly(L-lysine). After conjugation to all primary amine groups of the lysine residues through DOTA moieties, a polymeric micelle was obtained. The polymeric micelle-based MRI CA exhibited enhanced permeability and retention effect. A considerable amount of the polymeric micelle CA accumulated at solid tumors which doubled the MRI signal intensity [47].

Gadolinium can be prepared as hydrogel to be used as a CA in MRI. Gadolinium based nanohydrogel CA was prepared by incorporating Gd chelating cross-linkers into self-assembled pullulan nanogels to avoid repeated administration of CA and improve signal-to-noise ratios [48]. Effective and biosafe CA was prepared by attaching multiple Gd chelates to mesoporous silica nanoparticles (MSNs). The Gd³⁺ chelates were attached to the surface of dendrons via click chemistry. Resultant CA showed an approximately 11-fold increase in the relaxivity and enhancement of MR images [49].

3.4 Iron Oxide NPs

Typically, interaction between CAs and surrounding water protons typically originates and enhancement of MRI, which shorten the longitudinal (T1) or transverse (T2) relaxation time of nearby water molecules. Usually, T1 CAs are applied to increase signal intensity, resulting in a positive contrast enhancement (brighter image) in T1-weighted MRI, whereas T2 CAs can decrease signal intensity, providing a negative contrast enhancement (darker image) in T2-weighted MRI. Iron oxide NPs are generally considered safer than Gd-based CAs because iron is found in the human body, mostly stored as ferritin in the blood. Five unpaired electrons make Fe^{3+} a promising candidate for T1 CAs. Enhanced T1 contrast effects from small-sized iron oxide NP are obtained due to the presence of a large number of Fe^{3+} ions on the surface, which suppress T2 relaxation by their small magnetic moment [50].

The surface of iron oxide is rapidly oxidized by air so synthesized iron nanoparticles are not stable under aerobic atmosphere. Moreover, as synthesized, unmodified iron oxide NPs are not stable in vivo condition. Therefore, iron oxide NPs need to be coated. For instance, iron (Fe) core can be stabilized by controlling the surface oxidation using an oxygen transfer agent (i.e., trimethylamine *N*-oxide) [51]. Additionally, coating protects against iron oxide core agglomeration, provides chemical handles for the conjugation of targeting ligands, and avoids nonspecific cell interaction. A number of ways, including in situ coating, postsynthesis adsorption, and postsynthesis end grafting, can achieve coating [52]. Uniformly encapsulate coated cores are achieved in case of in situ and post synthesis modification with polysaccharides and copolymers whereas brush like extension anchored to the NP surface by the polymer end groups are obtained by grafting polymers (e.g., PEG). Alternatively, shell around the iron oxide core can be obtained using liposome and micelle-forming molecules for coating. Coating thickness and hydrophobicity are important as magnetic properties of the CAs are greatly affected by them [52, 53]. Thicker coatings can lower R2 relaxivities [53] and higher relaxivities can be obtained with hydrophilic coatings [54].

Iron oxide NPs can be made soluble in an aqueous solution using hydrophilic ligands with various anchoring groups, including carboxylic acids, catechol-based molecules (e.g., dopamine) [55], and bisphosphonates [56]. Silanization can be used for iron oxide materials. Iron oxide NPs was coated with a mixture of 3-aminopropylsilane (APS) and PEG-silane of different lengths by a ligand exchange reaction [57].

3.5 Quantum Dots

Quantum dots (QDs) is one of the most attractive nanomaterials in the biomedical fields due to their size-dependent tunable optical and electronic properties. Cell imaging is the main biological application of QDs. QDs can be categorized into two groups based on their cell biological applications such as nonspecific, and

cell-specific. Cell-specific and nonspecific mainly depend on the property of molecules recruited to the surface of QDs. Nonspecific extracellular and intracellular labeling can detect and image any cell type whereas biomarker specific targeted cell labeling is required for the detection and imaging of cancer cells and tumor milieu [58]. QDs are synthesized in the organic medium and are finished with highly hydrophobic aliphatic ligands such as alkyl phosphines, alkyl phosphine oxides, aliphatic amines, and aliphatic carboxylic acids. Therefore, ligand exchange reactions and surface modifications are necessary to make them suitable for biological applications.

Functionalizing semiconductor QD with biomolecules has some major challenges such as chemical instability in aqueous solutions, photo etching, toxicity due to the leaching out of cadmium ions, and unstable photoluminescence [59]. Surface coating with amphiphilic ligands or polymers can provide water soluble QDs. Ligand exchange, electrostatic adsorption, or covalent attachment are used for coupling small molecules or biomolecules to functional groups of polymer [60]. In another approach, Paquet et al. [61] produced biofunctionalized QDs by associating polyhistidine tags with Zn atoms present on the QD surface. Conjugation of growth hormones and antibodies with QDs is required for targeted labeling of cells. Low-cost alternatives such as hyaluronic acid and folic acid are also investigated [58].

3.6 Carbon Nanomaterials

Nowadays, carbon nanomaterials are emerging as an interesting class of nanostructures for biological imaging due to their favorable optoelectronic properties such as NIR fluorescence, photoluminescence and unique Raman signature [62]. Carbon nanotubes (CNT), graphene, carbon dots, and nanodiamonds are the main members of carbonaceous nanomaterials although some novel structures have been recently cited such as carbon nanohorns and nanoonions [63, 64]. However, as synthesized, these structures are hydrophobic and not biocompatible. Therefore, covalent or non-covalent conjugation of hydrophilic molecules to them is prerequisite to enable them for biological applications. In case of noncovalent conjugation which is mainly π - π stacking, and hydrophobic interactions, the optoelectronic properties of the functionalized carbon nanomaterials are not affected. Sonication with amphiphilic molecules or surfactants helps to disperse carbon nanomaterials. However, the resulting suspensions are toxic and thus generally not compatible with in vivo application. PEG-based surfactants are preferred for in vivo applications. In case of covalent conjugation of carbon nanomaterials, stable suspensions in water are possible to obtain. Cycloaddition and oxidation reactions have been tried to impart various functional groups to sp^2 carbon atoms. For example, oxidation by nitric acid generates carboxyl groups on the ends of CNTs, which can further react with a variety of functional groups. In addition, in situ reduction of aryl-diazonium salts or Diels-Alder cycloaddition, among other organic reactions, can be used to conjugate dyes, biomolecules, ligands, drugs, or other nanomaterials [65].

4 Organic Surface Coatings

4.1 Poly Ethylene Glycol (PEG)

Poly ethylene glycol (PEG) is a frequently used biocompatible linear synthetic polyether [66]. A low-molecular weight PEG is a clear, colorless, and viscous liquid. It is highly soluble with water and mostly soluble with alcohol and other organic solvents. Low-molecular weight PEG relatively low toxicity, which exhibited a good potential, and used in many cosmetic, nutraceutical, and pharmaceutical applications. Moreover, PEG can be prepared with a wide range of terminal functional groups as derivatives [67]. PEG along with its derivatives has been used clinically as excipients in FDA approved pharmaceutical formulations [68]. Being hydrophilic in biological fluids, PEG coating improve dispersity and blood circulation time of SPIONs [69]. PEG-coated (or PEGylated) SPIONs are not readily recognized by the reticuloendothelial system, hence, commonly regarded to as “stealth” nanoparticles [70]. This makes them suitable for target-specific cell labeling after modification with targeting ligands [71]. However, the same characteristic limits their use in imaging macrophages or other RES-related cells [72].

PEG polymers with molecular weight below 100,000 Da show amphiphilic characteristic and are soluble in water as well as in many organic solvents such as methylene chloride, ethanol, toluene, acetone, and chloroform. A variety of chemistries requiring the use of either aqueous or organic solvents are suitable for assembling at the SPION surface. For example, PEG can be coated onto SPIONs either by aqueous precipitation [73], or by grafting in the organic solvent (toluene) via a silane group [22]. Grafting in the organic solvent yielded a heterobifunctional PEG that have two ends. On end can be covalently attached to the SPION surface and the other end can be functionalized with targeting ligands, imaging reporter molecules, or therapeutic agents [18]. However, a PEG shell does not favor the uptake of SPIONs by most cells. Modification of the SPIONs with hyaluronic acid (HA) that act as a targeting moiety can solve this problem [74]. A recent study reported that different terminal groups of PEG could be used for fluorescence–MR dual-modality imaging guided cancer photothermal therapy [75].

4.2 Dextran

Dextran is a glycan composed of glucose subunits with a molecular weight ranging from 10 to 150 kDa. Its polar interactions (chelation and hydrogen bonding) provide a high affinity for iron oxide surfaces [76]. It is biocompatible as a result many of the clinically approved SPION preparations are dextran coated [77]. Molday and Mackenzie [78] first demonstrated the in situ coating preparation in 1982. Since then, different forms of dextran polymers such as carboxydextran and carboxymethyl dextran have been coated on SPIONs with varying hydrodynamic sizes [52].

Conventional dextran coatings are based on hydrogen bonding, which makes the polymer prone to detachment. However, cross-linked iron oxide (CLIO) can be a solution where coated polymers after SPION attachment are cross-linked using epichlorohydrin and ammonia [79]. Dextran coated CLIO nanoparticles were found to be a suitable platform for the synthesis of multifunctional imaging agents [80]. Although CLIOs improve circulation half-life in blood with no acute toxicity [81] due to the use of epichlorohydrin and their nonbiodegradability make them unsuitable for using in a clinical setting [82]. A multistep process using silane chemistry, which offer covalent bonding between dextran and SPION, can be an alternative of cross-linking [83].

4.3 Chitosan

Chitosan is a cationic, hydrophilic, and biodegradable natural polymer. It is derived by deacetylation of chitin obtained from the shells of crustaceans. Its large abundance in nature, ease of functionalization, biological activities, biocompatibility, high charge density, low toxicity toward mammalian cells, and ability to improve dissolution have made it a popular material for many biological applications [84]. Although chitosan and its derivatives have been used to develop polymeric nanoparticles through electrostatic complexation for decades [85], their use in magnetic nanoparticles is recent [86]. Direct and in situ coating of chitosan onto SPIONs is not easy as they are sparingly soluble at pH levels necessary to precipitate SPIONs [84]. However, chitosan-coated SPIONs was produced by adsorbing chitosan physically onto SPIONs coated with oleic acid which gave spherically shaped SPIONs with a diameter of 15 nm [87]. Chitosan-coated SPIONs can be used as gene delivery carrier in addition to CA due to the cationic nature of the chitosan that allows complexation with genetic material. For example, Bhattarai et al. [86] loaded anionic adenovirus vectors through electrostatic interactions on chitosan-coated SPIONs. These SPIONs showed enhanced gene transfection property. Moreover, chitosan possesses both amino and hydroxyl functional groups, which can be used for SPION functionalization with targeting, imaging, and therapeutic agents.

4.4 Liposomes and Micelles

Liposomes and micelles, spherical aggregates of amphiphilic molecules, are usually biocompatible as they are lipid bilayer of lamellar phase. Being bilayer structure liposomes can encapsulate SPIONs with resultant diameters ranging from 100 nm to 5 μm . Thus, liposome encapsulation can gather a certain number of MNPs for collective delivery to the target. For these reasons, liposome complexes become an ideal platform for delivery of contrast agents in MRI [88]. Liposomes and micelles coating can be done in two ways: postsynthesis incorporation or by in situ synthesizing. In the

first approach, water-soluble SPIONs can be attached to the aqueous center of the liposome [89], or alternatively, micelles can be coated around the structure to get hydrophobic SPIONs [90]. Second approach provides uniform NPs with a diameter of 15 nm where SPIONs can be precipitated in the liposomal core [91].

SPION coating with either liposomal or micellar structures has advantages over direct synthesis such as simple and easy surface modification, convenient encapsulation of pharmaceuticals inside the amphiphilic substructures, and chelation and protection of pharmaceuticals from the body until degraded in target cells [92]. However, there is a risk of coating agglomerates rather than discrete SPION cores in micellar or phospholipid structures, leading to poor physicochemical and magnetic properties [93].

4.5 Copolymers

Copolymers allow taking advantage of the distinct functionalities obtained from its constituents. Copolymer obtained by joining PEI and PEG polymers, can both form complex DNA to facilitate cell transfection (PEI functionality), and enable molecular targeting of cancer cells (PEG functionality) [94]. The advantages these copolymers provide can be applied to SPION coatings. For instance, a DNA delivering nanovector was developed, recently, by coating SPION with a copolymer of PEG-g-chitosan-g-PEI [95]. This study demonstrated that PEG, chitosan, and PEI polymers grafted together enabled the NP for DNA complexation, stabilization for in vivo use, and gene transfection. A unique pH-sensitive coating with a hydrophobic center layer was prepared using triblock PEG-poly(methacrylic acid)-poly(glycerol monomethacrylate) copolymer on SPIONs in situ. Coated NP was capable of encapsulating drug molecules and preferentially releasing the therapeutics in the acidic environment of the cellular endosome [96]. Similar copolymers were attach to the SPION surface by layer-by-layer deposition directed by matching of electrostatic interactions [97], hydrophilic/hydrophobic interactions [98], and covalently grafting polymer layers to base coatings [99].

5 Conclusion

Surface-functionalized NPs are extensively studied as CAs for MRI. This chapter mainly focuses on the surface modification of NPs such as silica NPs, gold NPs and quantum dots, carbon nanomaterials, and organic polymer coating including dextran, chitosan, PEG, copolymers through various bioconjugation reactions. Many biological applications of nanomaterials including imaging CAs, drug and gene delivery systems, biosensors, and nanomedicine share common functional groups, which are typically attached onto the surface of nanomaterials via suitable chemical or bioconjugation reaction to create nanofunctional nanodevices. However, that

there are some challenges and limitations including toxicity and biocompatibility is still a major issue to create nanomaterials using CAs for MRI application. Hence, multimodal and multifunctional NPs fabricated by the conjugation of various targeting molecules and CAs are extensively investigated for MRI on the way to treatment of cancer cells and tumors. Yet, controversial reports about toxicity and pharmacokinetics do not permit the clinical applications. Therefore, arguments of functionalized CAs that need to be addressed are biocompatibility, toxicity, in vivo and in vitro targeting efficiency, bioavailability, and renal and hepatobiliary clearance. The current scenario of research in the formulation and testing of CAs indicate that we may not to wait long for the complete transformation of conventional medicine into nanomedicine.

References

1. Smith, B. R., & Gambhir, S. S. (2017). Nanomaterials for in vivo imaging. *Chemical Reviews*, 117(3), 901–986. <https://doi.org/10.1021/acs.chemrev.6b00073>.
2. Na, H. B., & Hyeon, T. (2009). Nanostructured T1 MRI contrast agents. *Journal of Materials Chemistry*, 19(35), 6267–6273. <https://doi.org/10.1039/B902685A>.
3. Cao, Y., Xu, L., Kuang, Y., Xiong, D., & Pei, R. (2017). Gadolinium-based nanoscale MRI contrast agents for tumor imaging. *Journal of Materials Chemistry B*, 5(19), 3431–3461. <https://doi.org/10.1039/C7TB00382J>.
4. Lee, N., & Hyeon, T. (2012). Designed synthesis of uniformly sized iron oxide nanoparticles for efficient magnetic resonance imaging contrast agents. *Chemical Society Reviews*, 41(7), 2575–2589. <https://doi.org/10.1039/C1CS15248C>.
5. Hahn, M. A., Singh, A. K., Sharma, P., Brown, S. C., & Moudgil, B. M. (2011). Nanoparticles as contrast agents for in-vivo bioimaging: Current status and future perspectives. *Analytical and Bioanalytical Chemistry*, 399(1), 3–27. <https://doi.org/10.1007/s00216-010-4207-5>.
6. Merbach, A. S., Helm, L., & Toth, E. (2013). *The chemistry of contrast agents in medical magnetic resonance imaging*. Hoboken, NJ: Wiley.
7. Chan, K. W.-Y., & Wong, W.-T. (2007). Small molecular gadolinium(III) complexes as MRI contrast agents for diagnostic imaging. *Coordination Chemistry Reviews*, 251(17), 2428–2451. <https://doi.org/10.1016/j.ccr.2007.04.018>.
8. Weissleder, R., Kelly, K., Sun, E. Y., Shtatland, T., & Josephson, L. (2005). Cell-specific targeting of nanoparticles by multivalent attachment of small molecules. *Nature Biotechnology*, 23, 1418. <https://doi.org/10.1038/nbt1159>.
9. Veisoh, O., Kievit, F., Ellenbogen, R. G., & Zhang, M. (2011). Cancer cell invasion: Treatment and monitoring opportunities in nanomedicine. *Advanced Drug Delivery Reviews*, 63(8), 582–596. <https://doi.org/10.1016/j.addr.2011.01.010>.
10. Schellenberger, E. A., Weissleder, R., & Josephson, L. (2004b). Optimal modification of annexin V with fluorescent dyes. *Chembiochem: A European Journal of Chemical Biology*, 5(3), 271–274. <https://doi.org/10.1002/cbic.200300741>.
11. Lam, T., Avti, P. K., Pouliot, P., Maafi, F., Tardif, J. C., Rheume, E., Lesage, F., & Kakkar, A. (2016). Fabricating water dispersible superparamagnetic iron oxide nanoparticles for biomedical applications through ligand exchange and direct conjugation. *Nanomaterials*, 6(6), E100. <https://doi.org/10.3390/nano6060100>.
12. Sharpless, K. B., Finn, M. G., & Kolb, H. C. (2001). Click chemistry: Diverse chemical function from a few good reactions. *Angewandte Chemie (International ed in English)*, 40(11), 2004–2021. [https://doi.org/10.1002/1521-3773\(20010601\)40:11%3C2004::AID-ANIE2004%3E3.0.CO;2-5](https://doi.org/10.1002/1521-3773(20010601)40:11%3C2004::AID-ANIE2004%3E3.0.CO;2-5).

13. Lutz, J. F., & Zarafshani, Z. (2008). Efficient construction of therapeutics, bioconjugates, biomaterials and bioactive surfaces using azide-alkyne “click” chemistry. *Advanced Drug Delivery Reviews*, *60*(9), 958–970. <https://doi.org/10.1016/j.addr.2008.02.004>.
14. Hein, C. D., Liu, X. M., & Wang, D. (2008). Click chemistry, a powerful tool for pharmaceutical sciences. *Pharmaceutical Research*, *25*(10), 2216–2230. <https://doi.org/10.1007/s11095-008-9616-1>.
15. Sun, E. Y., Josephson, L., & Weissleder, R. (2006). “Clickable” nanoparticles for targeted imaging. *Molecular Imaging*, *5*(2), 122–128.
16. Maltzahn, v G., Ren, Y., Park, J.-H., Min, D.-H., Kotamraju, V. R., Jayakumar, J., Fogal, V., Sailor, M. J., Ruoslahti, E., & Bhatia, S. N. (2008). In vivo tumor cell targeting with “Click” nanoparticles. *Bioconjugate Chemistry*, *19*(8), 1570–1578. <https://doi.org/10.1021/bc800077y>.
17. Veiseh, O., Sun, C., Gunn, J., Kohler, N., Gabikian, P., Lee, D., Bhattarai, N., Ellenbogen, R., Sze, R., Hallahan, A., Olson, J., & Zhang, M. (2005). Optical and MRI multifunctional nanoprobe for targeting gliomas. *Nano Letters*, *5*(6), 1003–1008. <https://doi.org/10.1021/nl0502569>.
18. Conroy, S., Omid, V., Jonathan, G., Chen, F., Stacey, H., Donghoon, L., Raymond, S., Richard, G. E., Jim, O., & Miqin, Z. (2008). In vivo MRI detection of gliomas by chlorotoxin-conjugated superparamagnetic nanoprobe. *Small*, *4*(3), 372–379. <https://doi.org/10.1002/sml.200700784>.
19. Medarova, Z., Pham, W., Farrar, C., Petkova, V., & Moore, A. (2007). In vivo imaging of siRNA delivery and silencing in tumors. *Nature Medicine*, *13*, 372. <https://doi.org/10.1038/nm1486>.
20. Högemann, D., Josephson, L., Weissleder, R., & Basilion, J. P. (2000). Improvement of MRI probes to allow efficient detection of gene expression. *Bioconjugate Chemistry*, *11*(6), 941–946. <https://doi.org/10.1021/bc000079x>.
21. Schellenberger, E. A., Sosnovik, D., Weissleder, R., & Josephson, L. (2004a). Magneto/optical annexin V, a multimodal protein. *Bioconjugate Chemistry*, *15*(5), 1062–1067. <https://doi.org/10.1021/bc049905i>.
22. Kohler, N., Fryxell, G. E., & Zhang, M. (2004). A bifunctional poly(ethylene glycol) silane immobilized on metallic oxide-based nanoparticles for conjugation with cell targeting agents. *Journal of the American Chemical Society*, *126*(23), 7206–7211. <https://doi.org/10.1021/ja049195r>.
23. Wang, A. Z., Vaishali, B., Christophoros, V. C., Frank, G., Frank, A., Liangfang, Z., Mariam, S., Kai, Y., Michael, J. C., Robert, L., Philip, W. K., Neil, H. B., Sangyong, J., & Omid, C. F. (2008). Superparamagnetic iron oxide nanoparticle-aptamer bioconjugates for combined prostate cancer imaging and therapy. *ChemMedChem*, *3*(9), 1311–1315. <https://doi.org/10.1002/cmdc.200800091>.
24. Steitz, B., Hofmann, H., Kamau, S. W., Hassa, P. O., Hottiger, M. O., von Rechenberg, B., Hofmann-Amttenbrink, M., & Petri-Fink, A. (2007). Characterization of PEI-coated superparamagnetic iron oxide nanoparticles for transfection: Size distribution, colloidal properties and DNA interaction. *Journal of Magnetism and Magnetic Materials*, *311*(1), 300–305. <https://doi.org/10.1016/j.jmmm.2006.10.1194>.
25. Park, I.-K., Ng, C.-P., Wang, J., Chu, B., Yuan, C., Zhang, S., & Pun, S. H. (2008). Determination of nanoparticle vehicle unpackaging by MR imaging of a T(2) magnetic relaxation switch. *Biomaterials*, *29*(6), 724–732. <https://doi.org/10.1016/j.biomaterials.2007.10.018>.
26. Eyk, S., Jörg, S., Chris, R., Liset, U., Wolfdietrich, M., Matthias, T., & Bernd, H. (2008). Linking proteins with anionic nanoparticles via protamine: Ultrasmall protein-coupled probes for magnetic resonance imaging of apoptosis. *Small*, *4*(2), 225–230. <https://doi.org/10.1002/sml.200700847>.
27. Jain, T. K., Richey, J., Strand, M., Leslie-Pelecky, D. L., Flask, C. A., & Labhasetwar, V. (2008). Magnetic nanoparticles with dual functional properties: Drug delivery and magnetic resonance imaging. *Biomaterials*, *29*(29), 4012–4021. <https://doi.org/10.1016/j.biomaterials.2008.07.004>.

28. Pan, D., Caruthers, S. D., Hu, G., Senpan, A., Scott, M. J., Gaffney, P. J., Wickline, S. A., & Lanza, G. M. (2008). Ligand-directed nanobialys as theranostic agent for drug delivery and manganese-based magnetic resonance imaging of vascular targets. *Journal of the American Chemical Society*, *130*(29), 9186–9187. <https://doi.org/10.1021/ja801482d>.
29. Gunn, J., Wallen, H., Veiseh, O., Sun, C., Fang, C., Cao, J., Yee, C., & Zhang, M. (2008). A multimodal targeting nanoparticle for selectively labeling T cells. *Small*, *4*(6), 712–715. <https://doi.org/10.1002/sml.200701103>.
30. Wu, S.-H., Mou, C.-Y., & Lin, H.-P. (2013). Synthesis of mesoporous silica nanoparticles. *Chemical Society Reviews*, *42*(9), 3862–3875. <https://doi.org/10.1039/C3CS35405A>.
31. Yang, P., Gai, S., & Lin, J. (2012). Functionalized mesoporous silica materials for controlled drug delivery. *Chemical Society Reviews*, *41*(9), 3679–3698. <https://doi.org/10.1039/C2CS15308D>.
32. Tae-Jong, Y., Nam, Y. K., Eunha, K., Sung, K. J., Geol, K. B., Sang-Hyun, Y., Byeong-Hyeok, S., Myung-Haing, C., Jin-Kyu, L., & Bum, P. S. (2006). Specific targeting, cell sorting, and bioimaging with smart magnetic silica core-shell nanomaterials. *Small*, *2*(2), 209–215. <https://doi.org/10.1002/sml.200500360>.
33. Tallury, P., Payton, K., & Santra, S. (2008). Silica-based multimodal/multifunctional nanoparticles for bioimaging and biosensing applications. *Nanomedicine*, *3*(4), 579–592. <https://doi.org/10.2217/17435889.3.4.579>.
34. Koole, R., van Schooneveld, M. M., Hilhorst, J., Castermans, K., Cormode, D. P., Strijkers, G. J., de Mello Donegá, C., Vanmaekelbergh, D., Griffioen, A. W., Nicolay, K., Fayad, Z. A., Meijerink, A., & Mulder, W. J. M. (2008). Paramagnetic lipid-coated silica nanoparticles with a fluorescent quantum dot core: A new contrast agent platform for multimodality imaging. *Bioconjugate Chemistry*, *19*(12), 2471–2479. <https://doi.org/10.1021/bc800368x>.
35. Wang, F., Chen, X., Zhao, Z., Tang, S., Huang, X., Lin, C., Cai, C., & Zheng, N. (2011). Synthesis of magnetic, fluorescent and mesoporous core-shell-structured nanoparticles for imaging, targeting and photodynamic therapy. *Journal of Materials Chemistry*, *21*(30), 11244–11252. <https://doi.org/10.1039/C1JM10329F>.
36. Giersig, M., & Mulvaney, P. (1993). Preparation of ordered colloid monolayers by electrophoretic deposition. *Langmuir*, *9*(12), 3408–3413. <https://doi.org/10.1021/la00036a014>.
37. Haynes, W. M. (2014). *CRC handbook of chemistry and physics*. Boca Raton, FL: CRC.
38. Hou, W., Dasog, M., & Scott, R. W. J. (2009). Probing the relative stability of thiolate- and dithiolate-protected au monolayer-protected clusters. *Langmuir*, *25*(22), 12954–12961. <https://doi.org/10.1021/la9018053>.
39. Roux, S., Garcia, B., Bridot, J.-L., Salomé, M., Marquette, C., Lemelle, L., Gillet, P., Blum, L., Perriat, P., & Tillement, O. (2005). Synthesis, characterization of dihydrolipoic acid capped gold nanoparticles, and functionalization by the electroluminescent luminol. *Langmuir*, *21*(6), 2526–2536. <https://doi.org/10.1021/la048082i>.
40. Pérez-Rentero, S., Grijalvo, S., Peñuelas, G., Fàbrega, C., & Eritja, R. (2014). Thioctic acid derivatives as building blocks to incorporate DNA oligonucleotides onto gold nanoparticles. *Molecules*, *19*(7), 10495. <https://doi.org/10.3390/molecules190710495>.
41. Oh, E., Susumu, K., Mäkinen, A. J., Deschamps, J. R., Huston, A. L., & Medintz, I. L. (2013). Colloidal stability of gold nanoparticles coated with multithiol-poly(ethylene glycol) ligands: Importance of structural constraints of the sulfur anchoring groups. *The Journal of Physical Chemistry C*, *117*(37), 18947–18956. <https://doi.org/10.1021/jp405265u>.
42. Gehan, H., Fillaud, L., Felidj, N., Aubard, J., Lang, P., Chehimi, M. M., & Mangeney, C. (2010). A general approach combining diazonium salts and click chemistries for gold surface functionalization by nanoparticle assemblies. *Langmuir*, *26*(6), 3975–3980. <https://doi.org/10.1021/la9033436>.
43. WangWang, L. J., Fan, Q., Suzuki, M., Suzuki, I. S., Engelhard, M. H., Lin, Y., Kim, N., Wang, J. Q., & Zhong, C.-J. (2005). Monodispersed core-shell Fe₃O₄@Au nanoparticles. *The Journal of Physical Chemistry B*, *109*(46), 21593–21601. <https://doi.org/10.1021/jp0543429>.

44. Bao, J., Chen, W., Liu, T., Zhu, Y., Jin, P., Wang, L., Liu, J., Wei, Y., & Li, Y. (2007). Bifunctional Au-Fe₃O₄ nanoparticles for protein separation. *ACS Nano*, *1*(4), 293–298. <https://doi.org/10.1021/nn700189h>.
45. Fraum, T. J., Ludwig, D. R., Bashir, M. R., & Fowler, K. J. (2017). Gadolinium-based contrast agents: A comprehensive risk assessment. *Journal of Magnetic Resonance Imaging*, *46*(2), 338–353. <https://doi.org/10.1002/jmri.25625>.
46. Zhang, G., Zhang, R., Wen, X., Li, L., & Li, C. (2008). Micelles based on biodegradable poly(l-glutamic acid)-b-poly lactide with paramagnetic Gd ions chelated to the shell layer as a potential nanoscale MRI-visible delivery system. *Biomacromolecules*, *9*(1), 36–42. <https://doi.org/10.1021/bm700713p>.
47. Shiraiishi, K., Kawano, K., Minowa, T., Maitani, Y., & Yokoyama, M. (2009). Preparation and in vivo imaging of PEG-poly(L-lysine)-based polymeric micelle MRI contrast agents. *Journal of Controlled Release*, *136*(1), 14–20. <https://doi.org/10.1016/j.jconrel.2009.01.010>.
48. Chan, M., Lux, J., Nishimura, T., Akiyoshi, K., & Almutairi, A. (2015). Long-lasting and efficient tumor imaging using a high relaxivity polysaccharide nanogel magnetic resonance imaging contrast agent. *Biomacromolecules*, *16*(9), 2964–2971. <https://doi.org/10.1021/acs.biomac.5b00867>.
49. Guo, C., Hu, J., Bains, A., Pan, D., Luo, K., Li, N., & Gu, Z. (2016). The potential of peptide dendron functionalized and gadolinium loaded mesoporous silica nanoparticles as magnetic resonance imaging contrast agents. *Journal of Materials Chemistry B*, *4*(13), 2322–2331. <https://doi.org/10.1039/C5TB02709H>.
50. Zhang, H., Li, L., Liu, X. L., Jiao, J., Ng, C.-T., Yi, J. B., Luo, Y. E., Bay, B.-H., Zhao, L. Y., Peng, M. L., Gu, N., & Fan, H. M. (2017). Ultrasmall ferrite nanoparticles synthesized via dynamic simultaneous thermal decomposition for high-performance and multifunctional T1 magnetic resonance imaging contrast agent. *ACS Nano*, *11*(4), 3614–3631. <https://doi.org/10.1021/acsnano.6b07684>.
51. Peng, S., Wang, C., Xie, J., & Sun, S. (2006). Synthesis and stabilization of monodisperse Fe nanoparticles. *Journal of the American Chemical Society*, *128*(33), 10676–10677. <https://doi.org/10.1021/ja063969h>.
52. Laurent, S., Forge, D., Port, M., Roch, A., Robic, C., Vander Elst, L., & Muller, R. N. (2008). Magnetic iron oxide nanoparticles: Synthesis, stabilization, vectorization, physicochemical characterizations, and biological applications. *Chemical Reviews*, *108*(6), 2064–2110. <https://doi.org/10.1021/cr068445e>.
53. LaConte, L. E. W., Nitin, N., Zurkiya, O., Caruntu, D., O'Connor, C. J., Hu, X., & Bao, G. (2007). Coating thickness of magnetic iron oxide nanoparticles affects R2 relaxivity. *Journal of Magnetic Resonance Imaging*, *26*(6), 1634–1641. <https://doi.org/10.1002/jmri.21194>.
54. Duan, H., Kuang, M., Wang, X., Wang, Y. A., Mao, H., & Nie, S. (2008). Reexamining the effects of particle size and surface chemistry on the magnetic properties of iron oxide nanocrystals: New insights into spin disorder and proton relaxivity. *The Journal of Physical Chemistry C*, *112*(22), 8127–8131. <https://doi.org/10.1021/jp8029083>.
55. Gillich, T., Acikgöz, C., Isa, L., Schlüter, A. D., Spencer, N. D., & Textor, M. (2013). PEG-stabilized core-shell nanoparticles: Impact of linear versus dendritic polymer shell architecture on colloidal properties and the reversibility of temperature-induced aggregation. *ACS Nano*, *7*(1), 316–329. <https://doi.org/10.1021/nn304045q>.
56. Lalatonne, Y., Paris, C., Serfaty, J. M., Weinmann, P., Lecouvey, M., & Motte, L. (2008). Bisphosphonates-ultra small superparamagnetic iron oxide nanoparticles: A platform towards diagnosis and therapy. *Chemical Communications*, (22), 2553–2555. <https://doi.org/10.1039/B801911H>.
57. Barrera, C., Herrera, A. P., Bezares, N., Fachini, E., Olayo-Valles, R., Hinestroza, J. P., & Rinaldi, C. (2012). Effect of poly(ethylene oxide)-silane graft molecular weight on the colloidal properties of iron oxide nanoparticles for biomedical applications. *Journal of Colloid and Interface Science*, *377*(1), 40–50. <https://doi.org/10.1016/j.jcis.2012.03.050>.

58. Biju, V., Itoh, T., & Ishikawa, M. (2010). Delivering quantum dots to cells: Bioconjugated quantum dots for targeted and nonspecific extracellular and intracellular imaging. *Chemical Society Reviews*, 39(8), 3031–3056. <https://doi.org/10.1039/B926512K>.
59. Bilan, R., Fleury, F., Nabiev, I., & Sukhanova, A. (2015). Quantum dot surface chemistry and functionalization for cell targeting and imaging. *Bioconjugate Chemistry*, 26(4), 609–624. <https://doi.org/10.1021/acs.bioconjchem.5b00069>.
60. Banerjee, A., Gazon, C., Nadal, B., Pons, T., Krishnan, Y., & Dubertret, B. (2015). Fast, efficient, and stable conjugation of multiple DNA strands on colloidal quantum dots. *Bioconjugate Chemistry*, 26(8), 1582–1589. <https://doi.org/10.1021/acs.bioconjchem.5b00221>.
61. Paquet, C., Ryan, S., Zou, S., Kell, A., Tanha, J., Hulse, J., Tay, L.-L., & Simard, B. (2012). Multifunctional nanoprobe for pathogen-selective capture and detection. *Chemical Communications*, 48(4), 561–563. <https://doi.org/10.1039/C1CC16245D>.
62. Hong, G., Diao, S., Antaris, A. L., & Dai, H. (2015). Carbon nanomaterials for biological imaging and nanomedical therapy. *Chemical Reviews*, 115(19), 10816–10906. <https://doi.org/10.1021/acs.chemrev.5b00008>.
63. Karousis, N., Suarez-Martinez, I., Ewels, C. P., & Tagmatarchis, N. (2016). Structure, properties, functionalization, and applications of carbon nanohorns. *Chemical Reviews*, 116(8), 4850–4883. <https://doi.org/10.1021/acs.chemrev.5b00611>.
64. Marco, F., Roberto, M., Lyn, M., Kevin, F., Valentina, S., Giacomo, C., Luis, E., Eoin, M. S., & Silvia, G. (2015). Multi-functionalized carbon nano-onions as imaging probes for cancer cells. *Chemistry – A European Journal*, 21(52), 19071–19080. <https://doi.org/10.1002/chem.201503166>.
65. Biju, V. (2014). Chemical modifications and bioconjugate reactions of nanomaterials for sensing, imaging, drug delivery and therapy. *Chemical Society Reviews*, 43(3), 744–764. <https://doi.org/10.1039/C3CS60273G>.
66. Amstad, E., Zurcher, S., Mashaghi, A., Wong, J. Y., Textor, M., & Reimhult, E. (2009). Surface functionalization of single superparamagnetic iron oxide nanoparticles for targeted magnetic resonance imaging. *Small*, 5(11), 1334–1342. <https://doi.org/10.1002/sml.200801328>.
67. Mahato, R. I. (2004). *Biomaterials for delivery and targeting of proteins and nucleic acids*. Boca Raton, FL: CRC.
68. Fuertges, F., & Abuchowski, A. (1990). The clinical efficacy of poly(ethylene glycol)-modified proteins. *Journal of Controlled Release*, 11(1), 139–148. [https://doi.org/10.1016/0168-3659\(90\)90127-F](https://doi.org/10.1016/0168-3659(90)90127-F).
69. Xie, J., Xu, C., Kohler, N., Hou, Y., & Sun, S. (2007). Controlled PEGylation of monodisperse Fe₃O₄ nanoparticles for reduced non-specific uptake by macrophage cells. *Advanced Materials*, 19(20), 3163–3166. <https://doi.org/10.1002/adma.200701975>.
70. Harris, J. M., & Chess, R. B. (2003). Effect of pegylation on pharmaceuticals. *Nature Reviews Drug Discovery*, 2, 214. <https://doi.org/10.1038/nrd1033>.
71. Chen, X., Zhang, W., Laird, J., Hazen, S. L., & Salomon, R. G. (2008). Polyunsaturated phospholipids promote the oxidation and fragmentation of γ -hydroxyalkenals: Formation and reactions of oxidatively truncated ether phospholipids. *Journal of Lipid Research*, 49(4), 832–846. <https://doi.org/10.1194/jlr.M700598-JLR200>.
72. Papisov, M. I., Bogdanov, A., Schaffer, B., Nossiff, N., Shen, T., Weissleder, R., & Brady, T. J. (1993). Colloidal magnetic resonance contrast agents: Effect of particle surface on bio-distribution. *Journal of Magnetism and Magnetic Materials*, 122(1), 383–386. [https://doi.org/10.1016/0304-8853\(93\)91115-N](https://doi.org/10.1016/0304-8853(93)91115-N).
73. Lutz, J.-F., Stiller, S., Hoth, A., Kaufner, L., Pison, U., & Cartier, R. (2006). One-pot synthesis of PEGylated ultrasmall iron-oxide nanoparticles and their in vivo evaluation as magnetic resonance imaging contrast agents. *Biomacromolecules*, 7(11), 3132–3138. <https://doi.org/10.1021/bm0607527>.
74. Li, L., Jiang, W., Luo, K., Song, H., Lan, F., Wu, Y., & Gu, Z. (2013). Superparamagnetic iron oxide nanoparticles as MRI contrast agents for non-invasive stem cell labeling and tracking. *Theranostics*, 3(8), 595–615. <https://doi.org/10.7150/thno.5366>.

75. Ma, Y., Tong, S., Bao, G., Gao, C., & Dai, Z. (2013). Indocyanine green loaded SPIO nanoparticles with phospholipid-PEG coating for dual-modal imaging and photothermal therapy. *Biomaterials*, 34(31), 7706–7714. <https://doi.org/10.1016/j.biomaterials.2013.07.007>.
76. Tartaj, P., Morales, M. P., Veintemillas-Verdaguer, S., Gonzalez-Carreño, T., & Serna, C. J. (2006). Synthesis, properties and biomedical applications of magnetic nanoparticles. *Handbook of Magnetic Materials*, 16(5), 403–482.
77. Weissleder, R., Elizondo, G., Wittenberg, J., Lee, A. S., Josephson, L., & Brady, T. J. (1990). Ultrasmall superparamagnetic iron oxide: An intravenous contrast agent for assessing lymph nodes with MR imaging. *Radiology*, 175(2), 494–498. <https://doi.org/10.1148/radiology.175.2.2326475>.
78. Molday, R. S., & Mackenzie, D. (1982). Immunospecific ferromagnetic iron-dextran reagents for the labeling and magnetic separation of cells. *Journal of Immunological Methods*, 52(3), 353–367. [https://doi.org/10.1016/0022-1759\(82\)90007-2](https://doi.org/10.1016/0022-1759(82)90007-2).
79. Josephson, L., Tung, C.-H., Moore, A., & Weissleder, R. (1999). High-efficiency intracellular magnetic labeling with novel superparamagnetic-Tat peptide conjugates. *Bioconjugate Chemistry*, 10(2), 186–191. <https://doi.org/10.1021/bc980125h>.
80. Tassa, C., Shaw, S. Y., & Weissleder, R. (2011). Dextran-coated iron oxide nanoparticles: A versatile platform for targeted molecular imaging, molecular diagnostics, and therapy. *Accounts of Chemical Research*, 44(10), 842–852. <https://doi.org/10.1021/ar200084x>.
81. Wunderbaldinger, P., Josephson, L., & Weissleder, R. (2002). Crosslinked iron oxides (CLIO): A new platform for the development of targeted MR contrast agents. *Academic Radiology*, 9(Suppl 2), S304–S306.
82. McCarthy, J. R., & Weissleder, R. (2008). Multifunctional magnetic nanoparticles for targeted imaging and therapy. *Advanced Drug Delivery Reviews*, 60(11), 1241–1251. <https://doi.org/10.1016/j.addr.2008.03.014>.
83. Mornet, S., Portier, J., & Duguet, E. (2005). A method for synthesis and functionalization of ultrasmall superparamagnetic covalent carriers based on maghemite and dextran. *Journal of Magnetism and Magnetic Materials*, 293(1), 127–134. <https://doi.org/10.1016/j.jmmm.2005.01.053>.
84. Kumar, M. N. V. R., Muzzarelli, R. A. A., Muzzarelli, C., Sashiwa, H., & Domb, A. J. (2004). Chitosan chemistry and pharmaceutical perspectives. *Chemical Reviews*, 104(12), 6017–6084. <https://doi.org/10.1021/cr030441b>.
85. Janes, K. A., Calvo, P., & Alonso, M. J. (2001). Polysaccharide colloidal particles as delivery systems for macromolecules. *Advanced Drug Delivery Reviews*, 47(1), 83–97. [https://doi.org/10.1016/S0169-409X\(00\)00123-X](https://doi.org/10.1016/S0169-409X(00)00123-X).
86. Bhattarai, S. R., Kim, S. Y., Jang, K. Y., Lee, K. C., Yi, H. K., Lee, D. Y., Kim, H. Y., & Hwang, P. H. (2008). Laboratory formulated magnetic nanoparticles for enhancement of viral gene expression in suspension cell line. *Journal of Virological Methods*, 147(2), 213–218. <https://doi.org/10.1016/j.jviromet.2007.08.028>.
87. Hee Kim, E., Sook Lee, H., Kook Kwak, B., & Kim, B.-K. (2005). Synthesis of ferrofluid with magnetic nanoparticles by sonochemical method for MRI contrast agent. *Journal of Magnetism and Magnetic Materials*, 289, 328–330. <https://doi.org/10.1016/j.jmmm.2004.11.093>.
88. Kim, M.-J., Jang, D.-H., Lee, Y.-I., Jung, H. S., Lee, H.-J., & Choa, Y.-H. (2011). Preparation, characterization, cytotoxicity and drug release behavior of liposome-enveloped paclitaxel/Fe₃O₄ nanoparticles. *Journal of Nanoscience and Nanotechnology*, 11(1), 889–893. <https://doi.org/10.1166/jnn.2011.3267>.
89. Martina, M.-S., Fortin, J.-P., Ménager, C., Clément, O., Barratt, G., Grabielle-Madelmont, C., Gazeau, F., Cabuil, V., & Lesieur, S. (2005). Generation of superparamagnetic liposomes revealed as highly efficient MRI contrast agents for in vivo imaging. *Journal of the American Chemical Society*, 127(30), 10676–10685. <https://doi.org/10.1021/ja0516460>.

90. Yang, J., Lee, T.-I., Lee, J., Lim, E.-K., Hyung, W., Lee, C.-H., Song, Y. J., Suh, J.-S., Yoon, H.-G., Huh, Y.-M., & Haam, S. (2007). Synthesis of ultrasensitive magnetic resonance contrast agents for cancer imaging using PEG-fatty acid. *Chemistry of Materials*, *19*(16), 3870–3876. <https://doi.org/10.1021/cm070495s>.
91. De Cuyper, M., & Joniau, M. (1988). Magnetoliposomes. *European Biophysics Journal*, *15*(5), 311–319. <https://doi.org/10.1007/bf00256482>.
92. Mulder, W. J. M., Strijkers, G. J., van Tilborg, G. A. F., Griffioen, A. W., & Nicolay, K. (2006). Lipid-based nanoparticles for contrast-enhanced MRI and molecular imaging. *NMR in Biomedicine*, *19*(1), 142–164. <https://doi.org/10.1002/nbm.1011>.
93. Dagata, J. A., Farkas, N., Dennis, C. L., Shull, R. D., Hackley, V. A., Yang, C., Pirolo, K. F., & Chang, E. H. (2008). Physical characterization methods for iron oxide contrast agents encapsulated within a targeted liposome-based delivery system. *Nanotechnology*, *19*(30), 305101.
94. Veisheh, O., Kievit, F. M., Gunn, J. W., Ratner, B. D., & Zhang, M. (2009). A ligand-mediated nanovector for targeted gene delivery and transfection in cancer cells. *Biomaterials*, *30*(4), 649–657. <https://doi.org/10.1016/j.biomaterials.2008.10.003>.
95. Kievit, F. M., Veisheh, O., Bhattarai, N., Fang, C., Gunn, J. W., Lee, D., Ellenbogen, R. G., Olson, J. M., & Zhang, M. (2009). PEI-PEG-chitosan copolymer coated iron oxide nanoparticles for safe gene delivery: Synthesis, complexation, and transfection. *Advanced Functional Materials*, *19*(14), 2244–2251. <https://doi.org/10.1002/adfm.200801844>.
96. Guo, M., Yan, Y., Zhang, H., Yan, H., Cao, Y., Liu, K., Wan, S., Huang, J., & Yue, W. (2008). Magnetic and pH-responsive nanocarriers with multilayer core-shell architecture for anticancer drug delivery. *Journal of Materials Chemistry*, *18*(42), 5104–5112. <https://doi.org/10.1039/B810061F>.
97. Thünemann, A. F., Schütt, D., Kaufner, L., Pison, U., & Möhwald, H. (2006). Maghemite nanoparticles protectively coated with poly(ethylene imine) and poly(ethylene oxide)-block-poly(glutamic acid). *Langmuir*, *22*(5), 2351–2357. <https://doi.org/10.1021/la052990d>.
98. Bulte, J. W. M., de Cuyper, M., Despres, D., & Frank, J. A. (1999). Short- vs. long-circulating magnetoliposomes as bone marrow-seeking MR contrast agents. *Journal of Magnetic Resonance Imaging*, *9*(2), 329–335. [https://doi.org/10.1002/\(SICI\)1522-2586\(199902\)9:2<329::AID-JMRI27>3.0.CO;2-Z](https://doi.org/10.1002/(SICI)1522-2586(199902)9:2<329::AID-JMRI27>3.0.CO;2-Z).
99. Xiang, J. J., Tang, J. Q., Zhu, S. G., Nie, X. M., Lu, H. B., Shen, S. R., Li, X. L., Tang, K., Zhou, M., & Li, G. Y. (2003). IONP-PLL: A novel non-viral vector for efficient gene delivery. *The Journal of Gene Medicine*, *5*(9), 803–817. <https://doi.org/10.1002/jgm.419>.
100. Nicollay, K., Strijkers, G. and Grull, H. (2013). Gd-Containing Nanoparticles as MRI Contrast Agents. In *The Chemistry of Contrast Agents in Medical Magnetic Resonance Imaging* (eds A. Merbach, L. Helm and E. Toth). <https://doi.org/10.1002/9781118503652.ch11>.